Biodegradation (2012) 23:575–583
DOI 10.1007/s10532-012-9534-0

ORIGINAL PAPER

2,4,6-trichlorophenol (TCP) photobiodegradation and its effect on community structure

Yongming Zhang · Xuejing Pu · Miaomiao Fang · Jun Zhu · Lujun Chen · Bruce E. Rittmann

Received: 2 August 2011 / Accepted: 2 January 2012 / Published online: 20 January 2012

Abstract The mechanisms occurring in a photolytic circulating-bed biofilm reactor (PCBBR) treating 2,4,6-trichlorophenol (TCP) were investigated using batch experiments following three protocols: photodegradation alone (P), biodegradation alone (B), and intimately coupled photodegradation and biodegradation (P&B). Initially, the ceramic particles used as biofilm carriers rapidly adsorbed TCP, particularly in the B experiments. During the first 10 min, the TCP removal rate for P&B was equal to the sum of the rates for P and B, and P&B continued to have the greatest TCP removal, with the TCP concentration approaching zero only in the P&B experiments. When phenol, an easily biodegradable compound, was added along with TCP in order to promote TCP mineralization by means of secondary utilization, P&B was superior to P and B in terms of mineralization of TCP, giving 95% removal of chemical oxygen demand (COD). The microbial communities, examined by clone libraries, changed dramatically during the P&B experiments. Whereas *Burkholderia xenovorans,* a known degrader of chlorinated aromatics, was the dominant strain in the TCP-acclimated inoculum, it was replaced in the P&B biofilm by strains noted for biofilm formation and biodegrading non-chlorinated aromatics.

Keywords Biodegradation · Biofilm · Photolysis · Community structure · Trichlorophenol

Y. Zhang (✉) · X. Pu · M. Fang · J. Zhu
Department of Environmental Engineering, College of Life and Environmental Science, Shanghai Normal University, 200234 Shanghai, People's Republic of China
e-mail: zhym@shnu.edu.cn

L. Chen
School of Environment, Tsinghua University, 100084 Beijing, People's Republic of China

B. E. Rittmann
Swette Center for Environmental Biotechnology, Biodesign Institute, Arizona State University, Tempe, AZ 85287-5701, USA

Introduction

Trichlorophenol (TCP), one of most recalcitrant chlorinated phenols organics, is a main raw material for production of a wood-preservative agent, fungicides, defoliants, and herbicides (Chu and Law 2003; Tan et al. 2009; Jesús et al. 2009). TCP also is produced in the processes of pulp and paper bleaching and drinking water chlorination (Ali and Sreekrishnan 2001; Keith and Telliard 1979). Even more alarming is that TCP has been detected in soil, surface water, and even groundwater (Boyd S et al. 1989; Ramamoorthy 1997; Chang et al. 1999; Gardin et al. 2001) due to its widespread use in the production of a variety of biocides and as a biocide itself (Häggblom 1992). Because TCP is listed as one of the toxic pollutants most needing control (Xia and Zhang 1990; USEPA 1991), treatment of the polluted wastewater and ground water containing TCP has been a focus of

researchers around the world (Parra et al. 2002; Stafford et al. 1997; Marsolek et al. 2008).

Some advanced oxidation processes (AOPs) have been used for treatment of wastewater containing chlorophenols (Scott and Ollis 1995), e.g., UV irradiation, ozone, Fenton′s reagent, photolysis, and photocatalysis (Huang W et al. 2005; Tai and Jiang 2005; Rengaraj and Li 2006). Among them, photolysis is promising as a means to partly transform the complex structure of molecules like TCP into biodegradable products (Enriquez et al. 2004; Sakthivel et al. 2001). While photolysis alone is inefficient and uneconomic for full mineralization of TCP, biodegradation following partial photodegradation provides a practical means for complete mineralization.

Sequentially coupled photodegradation and biodegradation have been applied for the degradation of TCP (Reddy et al. 2004; Alinsafi et al. 2007; Manilal et al. 1992). The normal sequence is photolysis used as pretreatment before biodegradation. This approach is logical in that the microorganisms are protected from UV irradiation and hydroxyl free radicals present in photolysis. It is necessary to determine an optimal time ratio for photodegradation and biodegradation in the sequentially coupled process in order to optimize its efficiency. If the time of photolysis is too short, biodegradation will be inefficient, because the TCP is not made sufficiently biodegradable. If the photolysis time is too long, the process becomes uneconomical, since oxidation by photolysis is expensive (Suryaman et al. 2006).

Intimately coupling photodegradation and biodegradation is an approach to overcome the uncertainty inherent to sequential treatment. In intimate coupling, the advanced oxidation and biodegradation processes occur simultaneously in a single reactor so that biodegradable products generated by advanced oxidation can be immediately biodegraded (Marsolek et al. 2008). This overcomes the need to optimally match the times of each step. Intimate coupling was successfully demonstrated for the degradation of TCP and phenol by using a photo(cata)lytic circulating-bed biofilm reactor (PCBBR) (Marsolek et al. 2008; Zhang et al. 2010a) and an integrated photocatalytic-biological reactor (IPBR) (Zhang et al. 2010b). Microorganisms able to biodegrade the photocatalytic products survived well by being protected inside macropores of circulating carriers in the PCBBR and in a biodegradation zone separated from the photodegradation zone in the IPBR.

In this research, we took advantage of the fact that 2,4,6-TCP can be transformed by photolysis, thus eliminating the need to provide a photocatalyst. We investigated the mechanisms of 2,4,6-TCP degradation in a PCBBR using three batch protocols when photocatalyst was absent: photolysis alone (P), biodegradation alone (B), and intimately coupled photolysis and biodegradation (P&B). In the PCBBR, we used special light-weight, porous ceramic particles as biofilm carriers. In order to promote TCP mineralization, we added phenol as a means to accentuate secondary utilization (Namkung and Rittmann 1987a, b) of TCP in some experiments. We also examined the biofilm in the P&B carriers by means of genomics techniques to evaluate the impacts of intimately coupled photobiodegradation of 2,4,6-TCP on the community structure.

Materials and methods

Photolytic circulating-bed bioreactor (PCBBR)

The PCBBR was made of quartz glass with a working volume of 220 ml, and its configuration is the same as in Zhang et al. (2010a), as shown in Fig. 1a. Water and carriers circulated due to air-lift pumping created by aeration during the experiments. Ultraviolet light (254 nm wavelength) was provided from one side with a UV-light assembly consisting of 3 lamps with 8 W per lamp and having total power of 24 W. No TiO_2 photocatalyst was used in the experiments; thus, the reactions were photolytic, not photocatalytic.

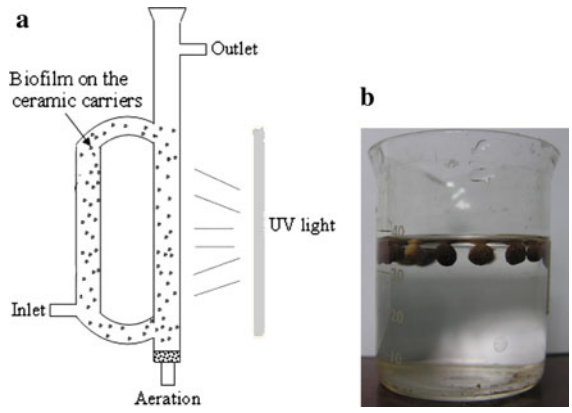

Fig. 1 Photolytic circulating-bed bioreactor (PCBBR) components. **a** Schematic of the PCBBR, **b** Light ceramic carriers floating in salt water with specific gravity of 1.1

Light-weight porous ceramic carrier

We produced a light-weight ceramic carrier from carborundum powder as the foaming agent. The powder was mixed thoroughly with light silicate, including kaoline and feldspar powders, at a weight ratio of 95–98% carborundum and 5–2% silicate. Then, the mixed powders were pressed to form a brick, dried at 100°C, and calcined at about 1200°C to produce a light-weight, porous ceramic solid. Calcining allowed the carborundum to expand at the melting point of the mixed powder, because the reactions of kaoline and feldspar produced gas that formed many pores. Some of these pores were closed inside the ceramic carrier when the temperature decreased, resulted in a specific gravity of 0.95. After the porous ceramic brick was broken into particles with diameters of 2–3 mm, the small particles were glazed and re-calcined at 600°C, which brought the specific gravity to 1.03–1.05, which is ideal for good circulation in the PCBBR. Figure 1b shows the carriers floating in salt water with specific gravity of 1.1.

Acclimation and incubation of 2,4,6-TCP-degrading bacteria

We obtained activated sludge from the underflow of a secondary clarifier at the Longhua municipal wastewater treatment plant in Shanghai. It was acclimated initially by adding phenol to an inorganic-salts medium at 20–25°C for the first two weeks, replacing the solution every day. The inorganic salt medium contained ammonium sulfate, 0.1 g/l; potassium dihydrogenphosphate, 0.5 g/l; disodium hydrogenphosphate, 0.5 g/l; magnesium sulfate, 0.5 g/l; and yeast extract, 0.02 g/l. The concentration of phenol was increased gradually from 50 to 300 mg/l during the first acclimation stage of two weeks, and the corresponding COD removal percentages was 50–60%. After two weeks, we replaced phenol with 2,4,6-TCP and continued acclimation for another two weeks. The same inorganic salts medium was used and replaced every day. The concentration of 2,4,6-TCP was increased gradually from 5 to 50 mg/l during the two-week acclimation.

TCP and synthetic wastewater

2,4,6-TCP was purchased from the Shanghai Sinopharm Chemical Reagent Co., Ltd. Synthetic wastewater was manufactured by adding 10–30 mg/l of 2,4,6-TCP and inorganic salts into tap water. The inorganic salts were the same as for acclimation.

Degradation of TCP

We employed three protocols, i.e. photolysis alone (P), biodegradation alone (B), and coupled photolysis and biodegradation (P&B), to evaluate TCP degradation in batch experiments. All experiments were carried out at room temperature (23–25°C). The UV light intensity was 0.46 mW/cm^2, corresponding to 24 W of UV light, for P and P&B experiments. Solutions including 2,4,6-TCP with concentration of 10, 15, 20, 25, or 30 mg/l were added to the PCBBR reactor to initiate the batch reactions. Solution circulation ($\sim$30 cycles per minute) was driven by aeration of 150 ml/min in the riser segment. Liquid samples were taken over time to analyze for the concentration of 2,4,6-TCP. We added 100 mg/l phenol to 20 mg/l TCP in order to promote TCP mineralization by means of secondary utilization in some experiments. During the experiments, the pH was not adjusted and maintained at approximately 7.0 with a phosphate buffer.

Control experiment

Adsorption of TCP to the ceramic carriers occurred, especially in the initial stage of a batch experiment. To assess TCP adsorption, we carried out control experiments using bare ceramic carriers and ceramic carriers with biofilm inactivated by heat sterilization by autoclaving.

Photodegradation (P)

The solutions were circulated with constant UV exposure, and no ceramic carriers were used in the P experiments.

Biodegradation (B)

Prior to the B batch tests, 10.6 g ceramic carriers were immersed into the acclimated activated sludge with 2,000 mg/l mixed liquor suspended solids (MLSS) for 24 h to let microorganism attach on the carriers. Then, we put the biofilm-colonized carriers into the reactor along with the synthetic wastewater including TCP. The biofilm-colonized ceramic carriers with biofilm

were circulated by aeration, but the UV light was off for the B experiments.

Intimately coupled photolysis and biodegradation (P&B)

The P&B experiments were run with the same biofilm-colonized carriers as in the B experiments. After the B experiments were completed, the carriers were retained, and the synthetic wastewater containing 2,4,6-TCP was applied to the PCBBR with the UV light on.

Analytical methods

2,4,6-TCP was measured by a high performance liquid chromatograph (HPLC, model: Agilent 1100, ASU) equipped with a diode array detector (DAD) with wavelength of 250 nm and ZORBAX SB-C18 column (5 μm, 4.6 × 150 mm). The mobile phase was a mixture of methanol:water solution (80:20, v/v), and the flow rate was 1 ml/min. The UV-light intensity was measured by an illuminometer (model: BG-2254, China) after filtration through a 0.45-μm cellulose acetate membrane filter.

The COD concentration was determined using potassium dichromate oxidation according to standard procedures (American Public Health Association (APHA) 2001) that involve providing a stoichiometric excess of potassium dichromate, strong acid and heating conditions, silver sulfate as a catalyst, and mercury sulfate to avoid the interference of chloride ion.

Community analysis

Acclimated activated sludge degrading 2,4,6-TCP was sample 1, and biofilm from the inside of the ceramic carriers after the P&B experiments was sample 2. The DNA of the microorganisms was extracted with DNAzol reagent and amplified through the PCR reaction (Godon et al. 1997); the reaction volume was 50 μl, including 29 Hotstart-PCR mix 25 μl, primers (25 pmol μ/l) 0.8 μl × 2, template 1 μl and ddH_2O 22.4 μl. The primers were 16S rRNA: 27F (5′-AGAGTTTGATCCTGGCTCAG-3′) and 630R (5′-CAKAAAGGAGGTGATCC-3′) (Kazuya et al. 1999). Conditions of PCR amplification were: an initial denaturation at 94°C for 4 min; 35 cycles of denaturation (30 s at 94°C), annealing (30 s at 50°C), and extension (1 min at 72°C); and a final extension at 72°C for 10 min. PCR products were analyzed on 1% agarose gel by electrophoresis and purified with a DNA purification kit (Dingguo Co. Ltd, Beijing). Target gene fragments were cloned into pMD-18 T-vector and transferred into *E. coli* DH5α. Then, the positive clones were sequenced (Jierui CO. LTD, Shanghai). We compared the obtained 16S rRNA sequences using the GenBank database based on Basic Local Alignment Search Tool (BLAST) and submitted these clone sequences to Genbank. Homologues were chosen based on an e-value less than 0.001.

Results and discussion

Control experiments

Figure 2 shows the results in the control experiments of 4 h, in which bare ceramic carriers gave about 70% loss of TCP (duplicate experiments), and the ceramic carriers with inactivated biofilm gave about 37% loss of TCP. The three experiments had similar trends of rapid adsorption in the first 10 min, followed by gradual continued adsorption. The lower adsorption by the biofilm-colonized carriers indicates that the carrier was active in adsorbing TCP, while the biofilm blocked adsorption sites.

Effect of the protocols on the TCP degradation rate

Figure 3 show TCP concentrations during the P, B, and P&B experiments with the different initial TCP concentrations (10, 15, 20, 25, and 30 mg/l). The most important finding is that TCP removal by P&B was

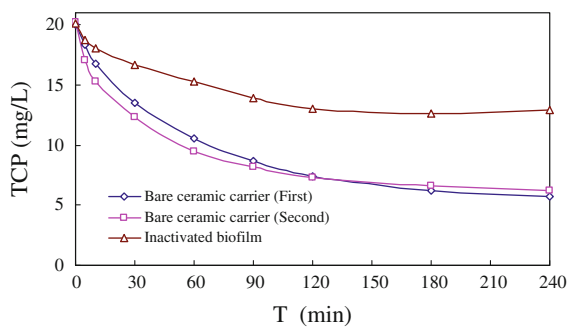

Fig. 2 Control experiments for evaluating TCP adsorption

substantially faster than by P and B for all starting concentrations. While TCP removals were greater in P than in B over the full 180-min experiment, B gave faster removal rates over the first 10 min, particularly for the higher TCP concentration, since adsorption was most active then (Fig. 2). In the B experiments in Fig. 3, TCP removal percentages for all initial TCP concentration over 3 h were greater than 37% (for inactivated biofilm, Fig. 2), which indicates that TCP was biodegraded, although the removal percentage was small compared to protocols P and P&B.

Figure 4a presents the average removal rates over the first 10 min (ARR = $(C_0–C)/t$, where C_0 and C are the initial and final TCP concentrations for the period of duration t (0–10 min in this case)). The initial TCP-removal rates increased with increasing initial TCP concentration in a linear manner. Furthermore, the initial rates by P&B were the sums of the rates by P and B. Since removal in the B experiment was dominated by adsorption in the first 10 min, the removal rate for P&B as the sum of adsorption and photolysis.

Figure 4b presents the TCP ARRs from 10 to 120 min, which was after adsorption stopped being the dominant mechanism in the B experiment, but before TCP disappeared in some of the P&B experiments. After 10 min, the removal rates in P were greater than by B, since photolysis reactions were able to continue for the entire experiment, while adsorption and biodegradation were slow in B. The fact that rates after 10 min were higher in P and P&B than in B underscores the value of having the photolysis reaction for a relatively recalcitrant molecule like TCP. Interestingly, the rates for the P&B experiments were

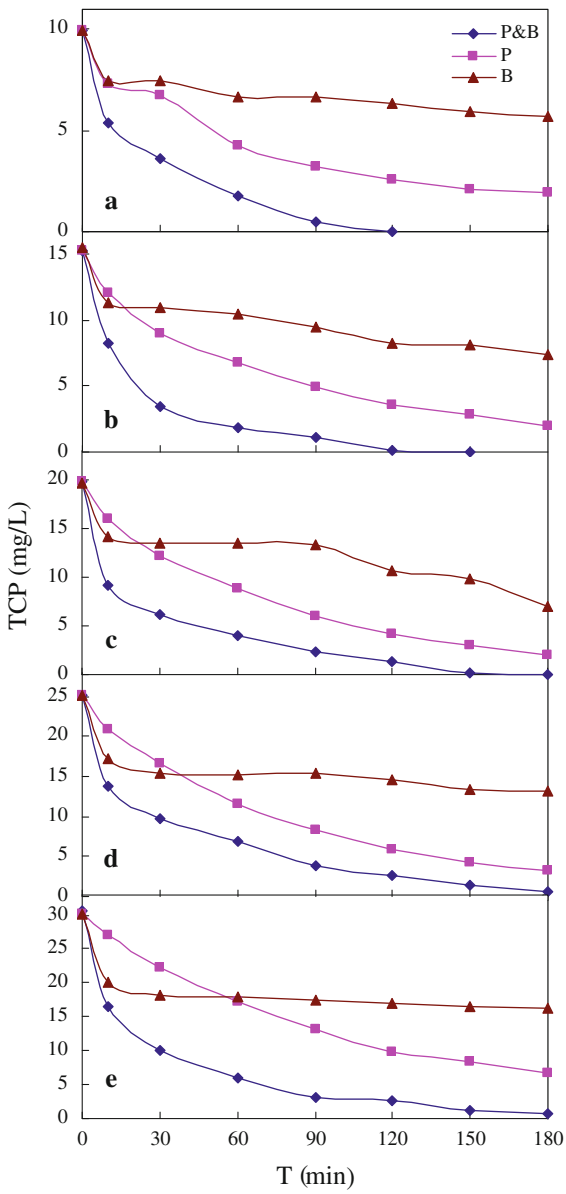

Fig. 3 TCP concentrations for the batch experiments corresponding to different protocols and initial TCP concentrations

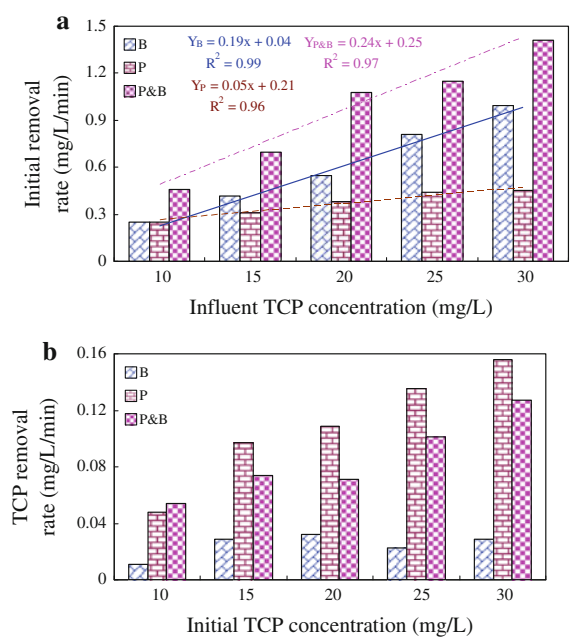

Fig. 4 Effect of protocols and initial TCP concentration on TCP average removal rates: **a** over the first 10 min, when adsorption dominated in B; and **b** for 10 min to 2 h

slower than for the P experiments after 10 min and when the initial TCP concentration was greater than 10 mg/l, although total TCP removal was the greatest. This phenomenon reflects that adsorption had made some of the TCP unavailable for photolysis.

Phenol promoted TCP mineralization by means of secondary utilization

COD removal is the index of the degree of TCP mineralization, but COD removal was minimal when TCP was the sole organic compound in the medium (data not shown). Therefore, additional batch experiments were carried out with 20 mg/l of TCP and 100 mg/l of phenol together; the addition of phenol was used to promote TCP mineralization through secondary utilization (Namkung and Rittmann 1987a, b; Aranda et al. 2003). Experiments were carried out with 100 mg/l of phenol alone (giving 239 mg/l COD) and 100 mg/l phenol plus 20 mg/l TCP (giving 258 mg/l COD).

Figure 5 summarizes the results for phenol and TCP degradation. After 3 h with the mixed solution, 100 mg/l phenol declined to 6, 0, and 0 mg/l in P, B, and P&B experiments, respectively (bottom panel in Fig. 4). With the mixture of phenol and TCP, degradation of phenol was slower than with phenol alone in the B and P&B experiments, perhaps due to inhibition by TCP. In the mixture experiment, the 20 mg/l TCP declined to 1.7, 1.5, and 0 mg/l in the P, B and P&B experiments, respectively, after one hour. Comparing the TCP panel in Fig. 5 with the middle panel of Fig. 3 clearly shows that the TCP removal rate was faster when phenol was added for B and P&B with the same initial TCP concentration of 20 mg/l. This result supports a secondary-utilization effect.

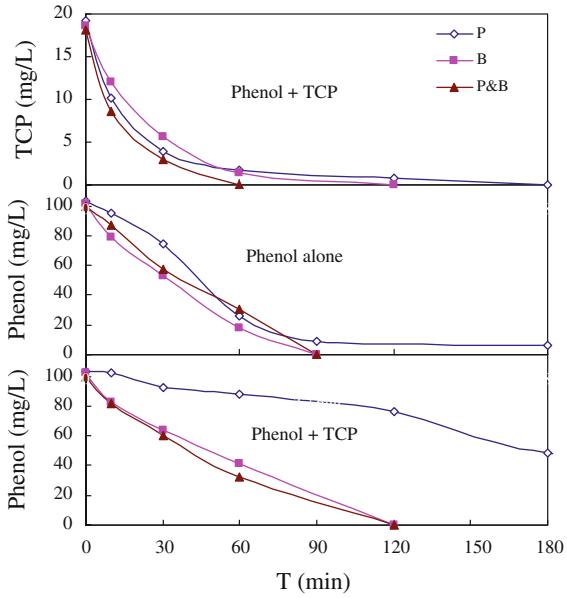

Fig. 5 Degradation of phenol with phenol alone (middle panel) and of phenol and TCP together (top and bottom panels) in P, B, and P&B batch experiments. The experiments were carried out with 100 mg/l of phenol alone or 100 mg/l phenol plus 20 mg/l TCP

Figure 6 shows the COD removals for 3 h in the same experiments. For the mixed solution, which had an initial COD of 258 mg/l, the COD removals were 42, 241, and 244 mg/l for P, B, and P&B experiments, respectively. COD removals contributed by phenol alone were 37, 225, and 226 mg/l from the starting COD of 239 mg/l. By difference, the COD removals for TCP degradation were 5, 16, and 18 mg/l for P, B, and P&B experiments, respectively. They constituted 26, 84, and 95 percent mineralizations of the 19 mg/l starting COD of TCP. Similar to TCP loss, the benefits of P&B treatment and of secondary utilization are evident for mineralization.

Community analysis

Genomic DNA extracted from samples 1 and 2 was PCR amplified and cloned into pMD18-T to build clone libraries. To characterize the flora composition, we sequenced 100 clones from each sample and analyzed them by BLAST search according to the GenBank database. Sample 1 (acclimated activated sludge) contained 29 unique strains (Table 1), while sample 2 (from the biofilm in the ceramic carriers after the P&B experiments) had 13 unique strains (Table 2).

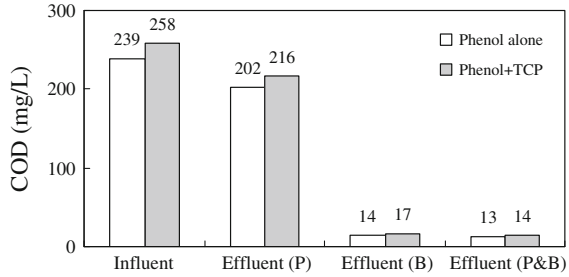

Fig. 6 COD removed for phenol alone and mixed phenol and TCP at 180 min

Table 1 Clone-library distributions of bacterial strains in the TCP-acclimated inoculum

Strain	Identity	Accession Number
Acidimicrobium ferrooxidans (2%)	90%	JN392922
Acidiphilium cryptum (1%)	90%	JF312870
Alkaliphilus metalliredigens (6%)	83%	JN392924
Anaeromyxobacter dehalogenans (6%)	86%	JN392925
Beijerinckia indica (2%)	91%	JF312873
Burkholderia xenovorans (35%)	96%	JN392928
Clostridium phytofermentans (1%)	83%	JN392931
Cytophaga hutchinsonii (1%)	85%	JF312877
Dehalococcoides sp. BAV1 (1%)	81%	JF312878
Desulfitobacterium hafniense (1%)	82%	JN392938
Flavobacterium johnsoniae (5%)	86%	JF312879
Gemmatimonas aurantiaca (1%)	85%	JF312880
Geobacter metallireducens (2%)	77%	JN392942
Kineococcus radiotolerans (2%)	87%	JN392944
Mesorhizobium sp. BNC1 (3%)	92%	JF312883
Methylibium petroleiphilum (5%)	97%	JF312884
Nitrosococcus oceani (1%)	89%	JN392947
Nitrosospira multiformis (1%)	90%	JF312885
Oligotropha carboxidovorans (1%)	98%	JF312886
Pedobacter heparinus (1%)	83%	JF312888
Pseudomonas fluorescens (3%)	98%	JF312891
Ralstonia eutropha (1%)	98%	JN392952
Rhodopirellula baltica (8%)	84%	JF312892
Novosphingobium aromaticivorans (4%)	98%	JN392948
Synechococcus (1%)	81%	JN392958
Syntrophus aciditrophicus (1%)	79%	JN392959
Thauera sp. MZ1T (2%)	97%	JF312895
Thioalkalivibrio (1%)	84%	JN392961

In sample 1 (Table 1), *Burkholderia xenovorans* had the greatest portion (35%), and no other strain was more than 8%. *Burkholderia xenovorans* strain LB400 can oxidize the biphenyl rings of PCB congeners, and it comes from a phylogenetic group that is commonly isolated from grass rhizospheres and soils with a variety of complex naturally occurring aromatic compounds (Bedard et al. 1986; Denef et al. 2004). Thus, *Burkholderia xenovorans* probably played a dominant role in biodegrading TCP in the acclimated activated sludge.

In sample 2 (Table 2), *Anoxybacillus flavithermus* (39%), *Novosphingobium aromaticivorans* (25%), and *Enterobacter* sp. 638 (18%) were the main strains, and

Table 2 Clone-library distributions of bacterial strains in the biofilm after the P&B experiments

Strain	Identity	Accession Number
Alkaliphilus metalliredigens (2%)	83%	JN392924
Anoxybacillus flavithermus (39%)	91%	JN392926
Burkholderia xenovorans (2%)	96%	JN392928
Dehalococcoides sp. BAV1 (1%)	81%	JF312878
Enterobacter sp. 638 (18%)	98%	JN392939
Erythrobacter litoralis (2%)	93%	JN392940
Flavobacterium johnsoniae (3%)	86%	JF312879
Kineococcus radiotolerans (1%)	87%	JN392944
Novosphingobium aromaticivorans (25%)	98%	JN392948
Paracoccus denitrificans (2%)	95%	JF312887
Pseudomonas fluorescens (3%)	98%	JF312891
Pseudomonas putida (1%)	96%	JN392950

B. xenovorans was only 2%. The most likely explanation for the large drop in *B. xenovorans* is that photolysis degraded TCP rapidly enough that *B. xenovorans* was out-competed for its substrate. The relatively slow rate of biodegradation compared to photolysis (Fig. 4b) supports this interpretation. *A. flavithermus* strain WK1 was isolated from a wastewater drain and could regulate biofilm formation in response to the environmental conditions (Saw J et al. 2008). *Novosphingobium* is a genus of Gram-negative bacteria that can degrade non-chlorinated aromatic compounds such as phenol, aniline, nitrobenzene, and phenanthrene (Liu et al. 2005; Sohn et al. 2004). *Enterobacter* sp. 638 is bacterium that resides within the living tissue of plants without substantively harming it. It can help their host plants to overcome the phytotoxic effects caused by environmental contamination (Barac et al. 2004). The numerical importance of *Anoxybacillus*, *Novosphingobium,* and *Enterobacter* suggests that they had advantages from good biofilm colonization of the carrier, feeding off photolysis products (such as dechlorinated aromatics), or both.

Conclusions

Compared with P and B, intimate coupling of P&B was obviously superior for 2,4,6-TCP removal due to the synergy between photolysis and biodegradation.

TCP mineralization could be realized by adding phenol to promote secondary utilization, with P&B giving 95% mineralization of TCP at the end of the 180-min experiment. In comparison, the P and B experiments gave 26 and 84% mineralizations of TCP, respectively. Clone libraries performed on the 16S rRNA sequences from samples of the TCP-acclimated inoculum to the PCBBR and from the biofilm carriers after the P&B experiments showed profound changes in the community. Whereas *Burkholderia xenovorans,* a known degrader of chlorinated aromatics, was the dominant strain in the inoculum, it was only 2% of the clones from the biofilm carriers. *B. xenovorans* was replaced by strains noted for biofilm formation and biodegrading non-chlorinated aromatics.

Acknowledgments The authors acknowledge the financial support by the National Natural Science Foundation of China (50978164 and 50678102), the Special Foundation of Chinese Colleges and Universities Doctoral Discipline (20070270003), the Shanghai Leading Academic Discipline Project (S30406), and the United States National Science Foundation (0651794).

References

Ali M, Sreekrishnan TR (2001) Aquatic toxicity from pulp and paper mill effluents: a review. Adv Environ Res 5(2):175–196

Alinsafi A, Evenou F, Abdulkarim EM, Pons MN, Zahraa O, Benhammou A, Yaacoubi A, Nejmeddine A (2007) Treatment of textile industry wastewater by supported photocatalysis. Dyes Pigm 74(2):439–445

American Public Health Association (APHA) (2001) Standard methods for the examination of water and wastewater, 22nd edn. American water works association and water pollution control federation, Washington

Aranda C, Godoy F, Becerra J, Barra R, Martínez M (2003) Aerobic secondary utilization of a non-growth and inhibitory substrate 2,4,6-trichlorophenol by *Sphingopyxis chilensis* S37 and *Sphingopyxis*-like strain S32. Biodegradation 14(4):265–274

Barac T, Taghavi S, Borremans B, Provoost A, Oeyen L, Colpaert JV, Vangronsveld J, van der Lelie D (2004) Engineered endophytic bacteria improve phytoremediation of water-soluble, volatile, organic pollutants. Nat Biotechnol 22(5):583–588

Bedard DL, Unterman R, Bopp LH, Brennan MJ, Haberl ML, Johnson C (1986) Rapid assay for screening and characterizing microorganisms for the ability to degrade polychlorinated biphenyls. Appl Environ Microbiol 51(4): 761–768

Boyd S A, Mikesell M D, Lee J (1989) Chlorophenols in soils. In: Reactions and movement of organic chemicals in soils. Soil Science Society of America and American Society of Agronomy, Madison, 209–228

Chang BV, Chiang CW, Yuan SY (1999) Microbial dechlorination of 2,4,6-trichlorophenol in anaerobic sewage sludge. Environ Sci Health B34:491–507

Chu W, Law CK (2003) Treatment of trichlorophenol by catalytic oxidation process. Water Res 37(10):2339–2346

Denef VJ, Park J, Tsoi TV, Rouillard JM, Zhang H, Wibbenmeyer JA, Verstraete W, Gulari E, Hashsham SA, Tiedje JM (2004) Biphenyl and benzoate metabolism in a genomic context: Outlining genome-wide metabolic networks in *Burkholderia xenovorans* LB400. Appl Environ Microbiol 70(8):4961–4970

Enriquez R, Beaugiraud B, Pichat P (2004) Mechanistic implications of the effect of TiO_2 accessibility in TiO_2-SiO_2 coatings upon chlorinated organics photocatalytic removal in water. Water Sci Technol 49(4):147–152

Gardin H, Lebeault JM, Pauss A (2001) Degradation of 2,4,6-trichlorophenol (2,4,6-TCP) by co-immobilization of anaerobic and aerobic microbial communities in an upflow reactor under air-limited conditions. Appl Microbiol Biotechnol 56(3–4):524–530

Godon JJ, Zumstein E, Dabert P, Habouzit FMR (1997) Molecular microbial diversity of an anaerobic digestor as determined by small-subunit r-DNA sequence analysis. Appl Environ Microbiol 63(7):2802–2813

Gómez-De Jesús A, Romano-Baez FJ, Leyva-Amezcua L, Juárez-Ramírez C, Ruiz-Ordaz N, Galíndez-Mayer J (2009) Biodegradation of 2,4,6-trichlorophenol in a packed-bed biofilm reactor equipped with an internal net draft tube riser for aeration and liquid circulation. J Hazard Mater 161(2–3):1140–1149

Häggblom MM (1992) Microbial breakdown of halogenated aromatic pesticides and related-compounds. FEMS Microbiol Rev 103(1):29–72

Huang WJ, Fang GC, Wang CC (2005) Ananometer-ZnO catalyst to enhance the ozonation of 2,4,6-trichlorophenol in water. Colloids Surf A 260(1–3):45–51

Kazuya W, Maki T, Shigeaki H (1999) An outbreak of non-flocculating catabolic populations caused the breakdown of a phenol-digesting activated-sludge process. Appl Environ Microbiol 65(7):2813–2819

Keith L, Telliard W (1979) Priority pollutants: I. a perspective view. Environ Sci Technol 13(4):416–423

Liu ZP, Wang BJ, Liu YH, Liu SJ (2005) *Novosphingobium taihuense* sp nov., a novel aromatic-compound-degrading bacterium isolated from Taihu Lake, China. Int J Sys Evol Microbiol 55(3):1229–1232

Manilal VB, Haridas A, Alexander R, Surender GD (1992) Photocatalytic treatment of toxic organics in wastewater: toxicity of photodegradation products. Water Res 26(8):1035–1038

Marsolek MD, Torres CI, Hausner M, Rittmann BE (2008) Intimate coupling of photocatalysis and biodegradation in a photocatalytic circulating-bed biofilm reactor. Biotechnol Bioeng 101(1):83–92

Namkung E, Rittmann BE (1987a) Modeling bisubstrate removal by biofilms. Biotechnol Bioeng 29(2):269–278

Namkung E, Rittmann BE (1987b) Evaluation of bisubstrate secondary utilization kinetics by biofilms. Biotechnol Bioeng 29(3):335–342

Parra S, Malato S, Pulgarin C (2002) New integrated photocatalytic-biological flow system using supported TiO_2 and

fixed bacteria for the mineralization of isoproturon. Appl Catal 36(2):131–144

Ramamoorthy S (1997) Chlorinated organic compounds in the environment. CRC Press, Boca Raton

Reddy MP, Srinivas B, Kumari VD, Subrahmanyam M, Sharma PN (2004) An integrated approach of solar photocatalytic and biological treatment of N-containing organic compounds in wastewater. Toxicol Environ Chem 86(1–4): 125–138

Rengaraj S, Li XZ (2006) Enhanced photocatalytic activity of TiO_2 by doping with Ag for degradation of 2,4,6-trichlorophenol in aqueous suspension. J Mol Catal 243(1):60–67

Sakthivel S, Neppolian B, Palanichamy M, Arabindoo B, Murugesan V (2001) Photocatalytic degradation of leather dye over ZnO catalyst supported on alumina and glass surfaces. Water Sci Technol 44(5):211–218

Saw JH, Mountain BW, Feng L, Omelchenko MV, Hou S, Saito JA, Stott MB, Li D, Zhao G, Wu J, Galperin MY, Koonin EV, Makarova KS, Wolf YI, Rigden DJ, Dunfield PF, Wang L, Alam M ((2008)) Encapsulated in silica: genome, proteome and physiology of the thermophilic bacterium Anoxybacillus flavithermus WK1. Genome Biol 9((11)): R161.1–R161.16

Scott JP, Ollis DF (1995) Integration of chemical and biological oxidation processes for water treatment; review and recommendations. Environ Prog 14(2):88–103

Sohn JH, Kwon KK, Kang JH, Jung HB, Kim SJ (2004) *Novosphingobium pentaromativorans* sp. nov., a high-molecular-mass polycyclic aromatic hydrocarbon-degrading bacterium isolated from estuarine sediment. Int J Sys Evol Microbiol 54(5):1483–1487

Stafford U, Kamat PV, Gray KA (1997) Photocatalytic degradation of 4-chlorophenol: the effects of varying TiO_2 concentration and light wavelength. J Catal 167(1):25–32

Suryaman D, Hasegawa K, Kagaya S (2006) Combined biological and photocatalytic treatment for the mineralization of phenol in water. Chemosphere 65(11):2502–2506

Tai C, Jiang GB (2005) Dechlorination and destruction of 2,4,6-trichlorophenol and pentachlorophenol using hydrogen peroxide as the oxidant catalyzed by molybdate ions under basic condition. Chemosphere 59(3):321–326

Tan IAW, Ahmad AL, Hameed BH (2009) Adsorption isotherms, kinetics, thermodynamics and desorption studies of 2,4,6-trichlorophenol on oil palm empty fruit bunch-based activated carbon. J Hazard Mater 164(2–3):473–482

USEPA (1991) Water quality criteria summary, ecological risk assessment branch (WH-585) and human risk assessment branch (WH-550D). Health and Ecological Criteria Division, USEPA, Washington

Xia Q, Zhang XH (1990) Manual on water quality standards. Environmental Science Press, Beijing

Zhang Y, Liu H, Shi W, Pu X, Rittmann BE (2010a) Photobiodegradation of phenol with ultraviolet irradiation of new ceramic biofilm carriers. Biodegradation 21(6): 881–887

Zhang YM, Wang L, Rittmann BE (2010b) Integrated photocatalytic-biological reactor for accelerated phenol degradation. Appl Microbiol Biotechnol 86(6):1977–1985